Purdue University
Purdue e-Pubs

International Compressor Engineering Conference

School of Mechanical Engineering

1976

Natural Frequencies and Modes of Gases in Multicylinder Compressor Manifolds and their use in Design

W. Soedel

J. M. Baum

NATURAL FREQUENCIES AND MODES OF GASES IN MULTI-CYLINDER COMPRESSOR MANIFOLDS AND THEIR USE IN DESIGN

Soedel, W. and Baum, J.M.
Ray W. Herrick Laboratories
Purdue University
West Lafayette, Indiana 47907

INTRODUCTION

In the following a case study of a four cylinder compressor is presented where particular attention is paid to the role that natural frequencies and modes play in the gas oscillations inside the compressor manifold.

The first part of the paper discusses the equation of motion of the gas that sloshes around in the manifold and concentrates then on the theoretical prediction of the natural frequencies and modes of the gas in the manifold. Typical results are shown.

The second part of the paper illustrates how knowledge of natural frequencies and modes can be used to predict (or explain) the occurence of large amplitude oscillations under certain conditions.

EQUATION OF MOTION

The equations of motion are derived using the Helmholtz resonator approach. This approach was presented in references [1,2] and will not be discussed here.

The example case is a four cylinder compressor with an eight degree of freedom discharge system in the vibration sense, not counting the discharge line which is taken as anechoic [3]. Referring to Figure 1, the elements labeled 1L, 1R, 2L, ..., etc. are considered the mass elements. Cavities 11, 12, 21, 22 ..., etc. represent the interconnecting springs between "plug" masses. The displacements of the plug masses are represented by the symbols ξ_{IJ} where the subscript J denotes that the plug is either to the right or to the left of the discharge cavity directly above the Ith cylinder. The acoustic displacement of a given plug is taken to be positive in the clockwise direction. This sign convention is used when the free body diagram and the equation of motion for a plug are written. The displacement of the gas at the entrance to the discharge pipe is ξ_p. This displacement is not analogous to the displacement of a "plug" mass because of the character of the anechoic termination assumed for the pipe where no sound waves are reflected back into the discharge cavity. It can be visualized as some function of the distance down the pipe from the entrance at any instant of time.

With this as background, we may proceed to derive the equations of motion for the system. They can be represented compactly by the matrix equation

$$[M]\ \{\ddot{\xi}\} + [C]\ \{\dot{\xi}\} + [K]\ \{\xi\} = \{S\Delta p\} \quad (1)$$

where

$[M]$ = mass matrix

$[C]$ = damping matrix

$[K]$ = stiffness matrix

ξ = plug displacement coordinate

$S\Delta p$ = force acting on plug

The damping matrix will be diagonal, including not only the anechoic termination effect, but also factors accounting for the energy loss due to friction. While in general the damping effect is very complex, a function of frequency of oscillation, fluid properties and geometric considerations, it is modeled for this compressor as an appropriate damping factor, after the fashion of single degree-of-freedom vibration problems. Thus, damping terms are of the form

$$C_{IJ} = \eta\ M_{IJ} \quad (2)$$

The mass matrix is diagonal except for the last row which represents the equation for the discharge pipe. Length terms L_{1L}, L_{1R}, L_{2L}, ... etc. do not represent physical lengths of the orifices between the cavities but are corrected lengths. Oscillatory fluid motion in the neck region was represented by a mass due to the dominance of the inertial over the compressible properties. Since the area of relatively high particle velocity extends beyond just the physical confines of the neck, an effective length for these masses must be determined. The effective length for a Helmholtz resonator neck is usually formulated as the geometric length plus an "end correction" to include the co-vibrating mass. Rayleigh [4] gives the end correction, ΔL for one end of a cylindrical plug, of length L and radius a, to be between the limits

$$0.79a < \Delta L < 0.85a \qquad (3)$$

For a hole in a thin wall, the lower limit is more correct while as the relative length of the plug increases, so does the end correction. For noncircular cross sections, it is suggested that the radius of a circle having the same cross-sectional area be used to find the end correction. Thus, for neck regions in the compressor cavity system, the effective length of plug 1L, for example is

$$L_{1L} = \text{geometric length neck 1L} + 2\left(0.82\sqrt{\frac{S_{1L}}{\pi}}\right) \qquad (4)$$

The force vector has terms of the form $S\Delta p$, the area times the difference in pressure between the cavities located at either side of the plug. Now, the cavities located far from the discharge pipe have higher mean thermodynamic pressures, over a cycle, than the ones nearer to the outlet so that mass moves toward and out the pipe. Thus, the pressure differential across any neck will not necessarily have an average value of zero over a cycle of the compressor but will be biased in the direction of mean mass flow. Since this bias appears in the equations of motion of the plugs as a constant force, the solution would yield ever increasing mean acoustic displacements. These displacements could give an acoustic pressure with a mean value. Since, the acoustic pressure was defined as a perturbation on mean pressure in the cavities which is described by the thermodynamic relationships, the proper force vector will be $S\Delta p_{avg}$ where the differential Δp_{avg} has an average value of zero over one compressor crank rotation.

Instead of using the displacements of the plug masses as the generalized coordinate, volume displacement, the cross-sectional area of the plug times its displacement, could be used. The solution of the equations for the volume displacement is more descriptive. It is the cavity volume change due to the plug oscillation which when multiplied by the spring constant for the cavity gives the change in cavity acoustic pressure due to the plug oscillation. Equation (1) could be rewritten as

$$[M]\{S\ddot{\xi}\} + [C]\{S\dot{\xi}\} + [K]\{S\xi\} = \{S\Delta p\} \qquad (5)$$

The elements in the matrices of equation (1) are shown in Figures 2, 3 and 4. Figure 5 gives the displacement and force vectors. Equation (1) can be solved along with the thermodynamic and valve dynamic equations by numerical integration.

NATURAL FREQUENCIES AND MODE SHAPES

The acoustic behavior of the compressor discharge network has been described by using analogous mechanical system elements of springs, masses and dampers. Thus, it is possible to obtain, just as with a mechanical system, a set of natural frequencies and modes. When excited by a harmonic force at one of these frequencies, the response, in the absence of damping, will become infinite. If however the response is initiated in some way at a natural frequency and forcing is immediately removed, the response will continue at that frequency with a particular pattern. This pattern, or mode shape, is unique to that frequency. In general, an 8-degree-of-freedom system will have 8 natural frequencies and associated mode shapes which may be found by reworking equation (1).

For undamped free vibration, equation (1) can be simplified to

$$[M']\{\ddot{\xi}\} + [K']\{\xi\} = 0 \qquad (6)$$

where

$$\underset{8\times8}{[M']} = \underset{9\times9}{[M]} \begin{array}{l}\text{Row 9 deleted}\\ \text{Column 9 deleted}\end{array} \qquad (7)$$

$$\underset{8\times8}{[K']} = \underset{9\times9}{[K]} \begin{array}{l}\text{Row 9 deleted}\\ \text{Column 9 deleted}\end{array} \qquad (8)$$

The deletions of row 9 and column 9 come about because elements in this row and this column describe the influence of the anechoic exit pipe. The influence of the anechoic discharge pipe is that of a damping element and is not considered in the eigenvalue analysis of the undamped system. However note, that if the pipe would not be anechoic, it could not any longer be deleted from the eigenvalue determination.

At a natural frequency, the response of the system will be harmonic

$$\{\xi\} = \{X\}\, e^{j\omega t} \qquad (9)$$

Substituting this into equation (6) yields

$$[[K'] - \omega^2 [M']]\{X\} = 0 \qquad (10)$$

This equation is satisfied if

$$\{X\} = 0 \qquad (11)$$

However, this solution is a case of no

interest. Another solution is found by letting the determinant of the matrix

$$[A] = [[K'] - \omega^2 [[M']] \qquad (12)$$

be zero:

$$|A| = 0 \qquad (13)$$

This is called the characteristic equation and represents the classical eigenvalue problem. It is solved for the natural frequencies, or eigenvalues. By substituting these eigenvalues into equation (10) one at a time, each eigenvector, or mode shape, may be found. The matrix [A] is given in Figure 6.

A program was written to generate the elements of the matrix, [A], and a library subroutine to solve the generalized eigenvalue problem, given by equation (13), was used. The following natural frequencies were obtained for the example case:

f_0 = 0 Hz	f_4 = 764 Hz
f_1 = 267 Hz	f_5 = 820 Hz
f_2 = 290 Hz	f_6 = 840 Hz
f_3 = 433 Hz	f_7 = 897 Hz

The numbers themselves are meaningless in the confines of this paper, since compressor dimensions are not defined. What is of interest is, that since none of the lumped elements is "fixed" to ground, a zero natural frequency exists. It corresponds to a rotational mode in which the masses move in a circle around the compressor axis so that they remain the same volume distance from each other with no "springs" stretched.

The first nonzero natural frequency has an acoustic displacement mode shape of

$$\{X\}_1 = \begin{Bmatrix} 1.00 \\ 1.80 \\ 1.81 \\ 1.47 \\ -1.09 \\ -1.87 \\ -1.76 \\ -1.37 \end{Bmatrix} \qquad (14)$$

with a corresponding volume displacement mode shape of

$$[SX]_1 = \begin{Bmatrix} 1.00 \\ 1.33 \\ 1.81 \\ 1.09 \\ -1.09 \\ -1.38 \\ -1.76 \\ -1.01 \end{Bmatrix} \qquad (15)$$

Again, the absolute numbers have no meaning attached. Only the character of the modes is of interest here.

Equation (14) gives the plug displacement at each of the mass locations, relative to $X_{1L} = 1$, for the response at 267 Hz. This can be visualized in Figure 7. As suggested previously when formulating equation (5), volume displacement is often a more interesting quantity since the change in cavity volume is proportional to the acoustic pressure in the cavity. So, the volume displacement mode shape for 267 Hz is shown in Figure 8.

Since $[S_{1R}\ X_{1R}]$ is greater than $[S_{1L}\ X_{1L}]$, there is an increase in the volume of cavity 11. Thus the "acoustic" pressure in the cavity is negative, denoted by a (-) in Figure 8. The relative magnitude of the pressure is given by

$$[p^a_{11}] = -\frac{c_d^2 \rho_d}{V_{11}} \left\{[S_{1L}\ X_{1L}] - [S_{1R}\ X_{1R}]\right\} \qquad (16)$$

Similar negative acoustic pressures exist in cavities 12, 41, and 42 while the acoustic pressure is positive in discharge cavities 21, 22, 31, and 32. Equations such as (16) can be formulated for the relative values of the other pressures. These constitute an acoustic pressure mode shape associated with the second natural frequency, and it is (normalized with respect to cavity 11)

$$\{p^a\}_1 = \begin{Bmatrix} 1.00 \\ 0.94 \\ -2.18 \\ -2.56 \\ -0.88 \\ -0.48 \\ 2.27 \\ 2.55 \end{Bmatrix} \qquad (17)$$

Figure 9 is a sketch meant to represent the mode shape given by equation (17). Here again, the length of the arrows correspond to the relative magnitude of the pressure in the cavities. Outward pointing arrows represent a pressure increasing with acoustic pressure 11 while an arrow pointing toward the center represents a cavity pressure which is negative when the pressure in cavity 11 is positive. For instance, if the system were excited at 267 Hz with forcing such that the acoustic pressure in cavity 11 is 2 psi, then the response in cavity 12 is 1.88 psi while in cavity 21 it will be out of phase with p^a_{11} with a magnitude of 4.36 psi. Also, if this mode was the dominant mode excited at some other frequency, one might expect that the acoustic pressure in cavities 21, 22, 41 and 42 would be larger than the fluctuating pressures in the other cavities.

The acoustic pressure mode shapes for the other frequencies are shown in Figure 10 and are

$$\{p^a\}_2 = \begin{Bmatrix} 1.00 \\ 1.13 \\ 0.67 \\ 0.33 \\ -0.86 \\ -1.19 \\ -0.44 \\ 0.06 \end{Bmatrix} \qquad \{p^a\}_3 = \begin{Bmatrix} 1 \\ -156 \\ -89 \\ 101 \\ 36 \\ -97 \\ -16 \\ 117 \end{Bmatrix}$$

$$\{p^a\}_4 = \begin{Bmatrix} 1.00 \\ 0.26 \\ -0.66 \\ 0.28 \\ 0.95 \\ 0.30 \\ -1.01 \\ -0.28 \end{Bmatrix} \qquad \{p^a\}_5 = \begin{Bmatrix} 1.00 \\ 0.05 \\ -0.42 \\ 0.39 \\ -1.05 \\ 0.03 \\ 0.28 \\ -0.40 \end{Bmatrix} \quad (18)$$

$$\{p^a\}_6 = \begin{Bmatrix} 1.00 \\ 2.14 \\ -3.57 \\ -0.97 \\ 4.30 \\ -3.00 \\ 7.39 \\ -4.93 \end{Bmatrix} \qquad \{p^a\}_7 = \begin{Bmatrix} 1.00 \\ -1.04 \\ 1.56 \\ -0.25 \\ 0.62 \\ -0.23 \\ 0.40 \\ -0.33 \end{Bmatrix}$$

HOW TO USE NATURAL FREQUENCY AND MODE INFORMATION IN DESIGN

To dramatize the use of natural frequency and mode information in design, let us not only look at compressors that run at nearly constant speed, like refrigeration compressors for appliance type applications, but rather at compressors that experience a large crankspeed range, like for instance in automotive applications.

For a typical compressor of this type (exact dimensions and parameters are of no importance in this example), we will get gas oscillations that are much larger in amplitude at certain crankspeeds than normally expected. For instance, simulation results taken at three speeds show small amplitude oscillations at 1000 RPM, medium activity at 3000 RPM and very pronounced oscillations at 5500 RPM (Figure 11).

The speeds at which large oscillations occur can be predicted, without running a complete simulation model which is relatively costly and laborsome, by generating from the natural frequency data a table that lists critical crankspeeds in descending order of importance as function of the discharge system natural frequency that is excited and the multiple of the crank speed that does the exciting. It can be shown from mathematical considerations, that as lower the harmonic number defining the multiple of the crankspeed is, as more pronounced in an amplitude sense will be in general the gas oscillations at that crankspeed. This applies for the frequency range that is of interest for thermodynamic performance. Especially severe are cases where there are not only low harmonic numbers, but where the mode number is low also. For the example case, the table is given as Figure 12.

The table is generated by realizing that whenever

$$\frac{m\,N}{60} = f_n \qquad (19)$$

we excite a natural mode. In this formula

N = crankspeed [RPM]

$m = 1, 2, \ldots, \infty$ and is the harmonic number

f_n = natural frequency

$n = 0, 1, 2, \ldots$ and indicates the natural mode and frequency as subscript

To make sure that no important crankspeed gets forgotten, it is best to list natural frequencies across and harmonic numbers down. For every combination, the value of N is obtained from Equation (19). The reason that some N values are blanked out is that for the example case 6000 RPM was the upper speed limit.

Let us now use the table. According to it we indeed expect large oscillation amplitudes in the vicinity of 5500 RPM. To be exact, at: 5380 and 5802 RPM. The example illustrates that one does not necessarily have to hit the critical speeds exactly. Coupling of the natural modes due to damping effects will spread the area in which to expect large amplitude oscillations.

Natural modes are another important piece of information for the designer. Those modes whose shape is encouraged by the particular phasing of the pistons will be excited stronger than mode shapes that are not encouraged by the piston phasing. This mode shape encouragement can override the harmonic number criteria outlined before in certain cases. Thus, if in the four cylinder piston case each pair of opposing cylinders discharges out of phase while the two pairs are $\frac{\pi}{2}$ radians crank angle out of phase, the modes associated with f_1, f_2 and f_5 will be encouraged, that is, excited more, while the modes associated with f_3, f_4, f_6 and f_7 will be discouraged, that is, excited less.

Thus, the recommended procedure is to:

1. Obtain natural frequencies and modes of discharge and suction systems either theoretically as shown in this

paper, or experimentally.

2. Generate a table as discussed before. (Note that if the compressor runs more or less at a constant speed, you have to generate the table only for a relatively narrow speed range.)

3. Investigate if a low harmonic number occurs.

4. Change natural frequencies of system, if necessary, by changing neck dimensions or volume sizes.

5. Investigate the piston phasing of the natural mode shapes. Change phasing, if necessary and feasible.

SUMMARY

A case study of a discharge manifold system for a four cylinder compressor was presented where particular attention was given to the role of natural frequencies and modes in the gas oscillation behavior.

The paper presented the equations of motion and showed how natural frequencies and modes were found for the example case.

It discussed the use of this information in design.

REFERENCES

1. Soedel, W., Padilla-Navas, E., and Kotalik, B.D., "On Helmholtz Resonator Effects in the Discharge System of a Two Cylinder Compressor," Journal of Sound and Vibration, Vol. 30, No. 3, 1973, pp. 263-277.

2. Soedel, W., "On Discretized Modeling of Flow Pulsations in Multi-Cylinder Gas Machinery Manifolds," Proceedings of the Conference on Vibrations and Noise in Pump, Fan, and Compressor Installations, The Institution of Mechanical Engineers, England, 1975.

3. Soedel, W., "On the Simulation of Anechoic Pipes in Helmholtz Resonator Models of Compressor Discharge Systems," Proceedings of the 1974 Purdue Compressor Technology Conference, Purdue University, West Lafayette, Indiana pp. 136-139.

4. Rayleigh, J.W.S., "Theory of Sound," Vol. II. Dover Publications, New York, 1945.

NOMENCLATURE

M = mass matrix terms (N sec^2/m]

C = damping matrix terms [N sec/m]

K = stiffness matrix terms [N/m]

ξ = "plug" displacements [m]

S = effective "plug" area [m^2]

Δp = pressure differential across "plug" [N/m^2]

η = damping coefficient [1/sec]

ω = frequency [rad/sec]

ΔL = end correction [m]

L = "plug" length

f_n = natural frequency [1/sec]

X = natural mode [m]

p^a = pressure with respect to mean pressure [N/m^2]

c_d = speed of sound at mean discharge pressure [m/sec]

ρ_d = mean discharge density [N sec^2/m^4]

N = crankspeed [RPM]

m = harmonic number

n = natural frequency and mode number

V = volumes [m^3]

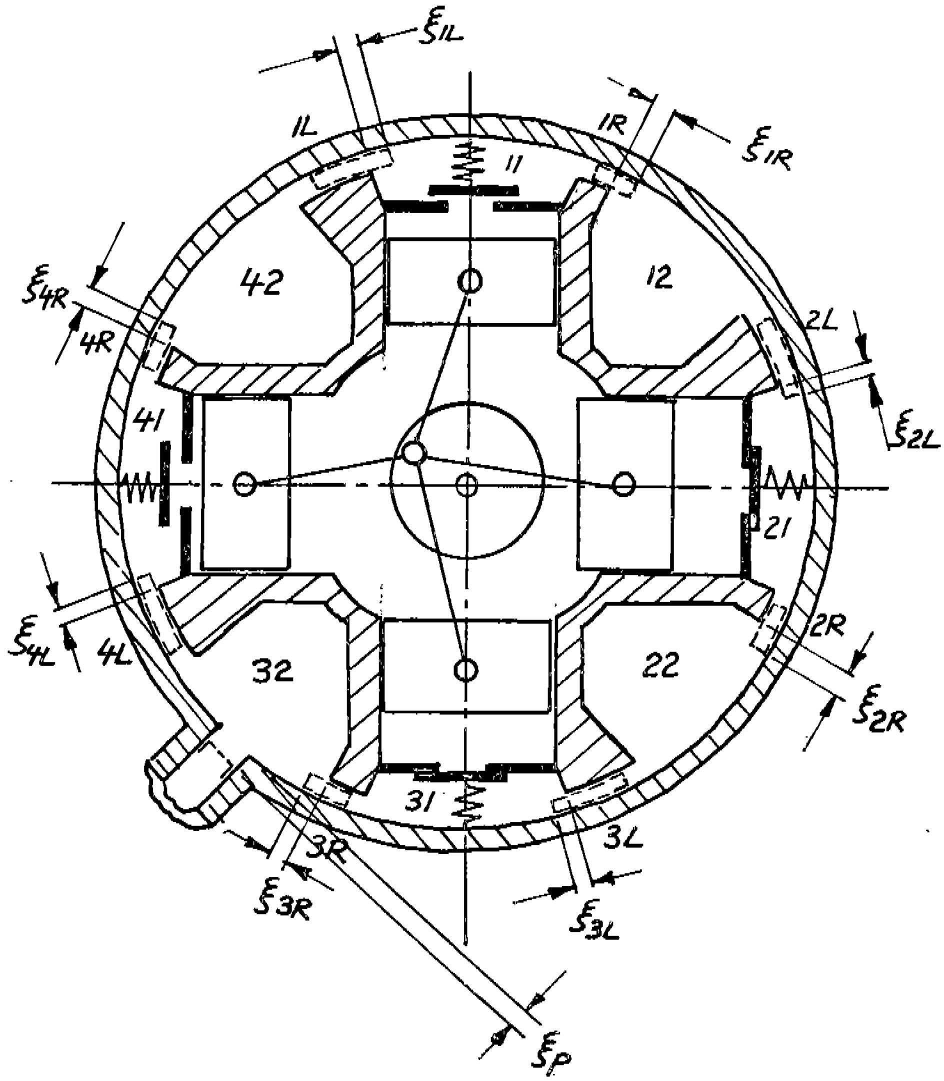

Figure 1 Discharge System

$$
\rho_d \begin{bmatrix}
L_{1L}S_{1L} & 0 & 0 & 0 & 0 & 0 & 0 & 0 & 0 \\
0 & L_{1R}S_{1R} & 0 & 0 & 0 & 0 & 0 & 0 & 0 \\
0 & 0 & L_{2L}S_{2L} & 0 & 0 & 0 & 0 & 0 & 0 \\
0 & 0 & 0 & L_{2R}S_{2R} & 0 & 0 & 0 & 0 & 0 \\
0 & 0 & 0 & 0 & L_{3L}S_{3L} & 0 & 0 & 0 & 0 \\
0 & 0 & 0 & 0 & 0 & L_{3R}S_{3R} & 0 & 0 & 0 \\
0 & 0 & 0 & 0 & 0 & 0 & L_{4L}S_{4L} & 0 & 0 \\
0 & 0 & 0 & 0 & 0 & 0 & 0 & L_{4R}S_{4R} & 0 \\
0 & 0 & 0 & 0 & 0 & 0 & 0 & 0 & 0
\end{bmatrix}
$$

Figure 2 Mass Matrix

$$
\rho_d c_d^2
\begin{bmatrix}
S_{1L}^2\left(\frac{1}{V_{42}}+\frac{1}{V_{11}}\right) & -\frac{S_{1L}S_{1R}}{V_{11}} & 0 & 0 & 0 & 0 & 0 & -\frac{S_{1L}S_{4R}}{V_{42}} & 0 \\
-\frac{S_{1R}S_{1L}}{V_{11}} & S_{1R}^2\left(\frac{1}{V_{11}}+\frac{1}{V_{12}}\right) & -\frac{S_{1R}S_{2L}}{V_{12}} & 0 & 0 & 0 & 0 & 0 & 0 \\
0 & -\frac{S_{2L}S_{1R}}{V_{12}} & S_{2L}^2\left(\frac{1}{V_{12}}+\frac{1}{V_{21}}\right) & -\frac{S_{2L}S_{2R}}{V_{21}} & 0 & 0 & 0 & 0 & 0 \\
0 & 0 & -\frac{S_{2R}S_{2L}}{V_{21}} & S_{2R}^2\left(\frac{1}{V_{21}}+\frac{1}{V_{22}}\right) & -\frac{S_{2R}S_{3L}}{V_{22}} & 0 & 0 & 0 & 0 \\
0 & 0 & 0 & -\frac{S_{3L}S_{2R}}{V_{22}} & S_{3L}^2\left(\frac{1}{V_{22}}+\frac{1}{V_{31}}\right) & -\frac{S_{3L}S_{3R}}{V_{31}} & 0 & 0 & 0 \\
0 & 0 & 0 & 0 & -\frac{S_{3R}S_{3L}}{V_{31}} & S_{3R}^2\left(\frac{1}{V_{31}}+\frac{1}{V_{32}}\right) & -\frac{S_{3R}S_{4L}}{V_{32}} & 0 & -\frac{S_{3R}S_p}{V_{32}} \\
0 & 0 & 0 & 0 & 0 & -\frac{S_{4L}S_{3R}}{V_{32}} & S_{4L}^2\left(\frac{1}{V_{32}}+\frac{1}{V_{41}}\right) & -\frac{S_{4L}S_{4R}}{V_{41}} & \frac{S_{4L}S_p}{V_{32}} \\
-\frac{S_{4R}S_{1L}}{V_{42}} & 0 & 0 & 0 & 0 & 0 & -\frac{S_{4R}S_{4L}}{V_{41}} & S_{4R}^2\left(\frac{1}{V_{41}}+\frac{1}{V_{42}}\right) & 0 \\
0 & 0 & 0 & 0 & 0 & -\frac{S_p S_{3R}}{V_{32}} & \frac{S_p S_{4L}}{V_{32}} & 0 & \frac{S_p^2}{V_{32}}
\end{bmatrix}
$$

Figure 3 Stiffness Matrix

$$
g_d \begin{bmatrix}
\eta L_{1L} S_{1L} & 0 & 0 & 0 & 0 & 0 & 0 & 0 & 0 \\
0 & \eta L_{1R} S_{1R} & 0 & 0 & 0 & 0 & 0 & 0 & 0 \\
0 & 0 & \eta L_{2L} S_{2L} & 0 & 0 & 0 & 0 & 0 & 0 \\
0 & 0 & 0 & \eta L_{2R} S_{2R} & 0 & 0 & 0 & 0 & 0 \\
0 & 0 & 0 & 0 & \eta L_{3L} S_{3L} & 0 & 0 & 0 & 0 \\
0 & 0 & 0 & 0 & 0 & \eta L_{3R} S_{3R} & 0 & 0 & 0 \\
0 & 0 & 0 & 0 & 0 & 0 & \eta L_{4L} S_{4L} & 0 & 0 \\
0 & 0 & 0 & 0 & 0 & 0 & 0 & \eta L_{4R} S_{4R} & 0 \\
0 & 0 & 0 & 0 & 0 & 0 & 0 & 0 & c_d S_P
\end{bmatrix}
$$

Figure 4 Damping Matrix

$$\{S\Delta p\} = \left\{\begin{array}{|c|} \hline S_{1L}(p_{42}-p_{11}) \\ \hline S_{1R}(p_{11}-p_{12}) \\ \hline S_{2L}(p_{12}-p_{21}) \\ \hline S_{2R}(p_{21}-p_{22}) \\ \hline S_{3L}(p_{22}-p_{31}) \\ \hline S_{3R}(p_{31}-p_{32}) \\ \hline S_{4L}(p_{32}-p_{41}) \\ \hline S_{4R}(p_{41}-p_{42}) \\ \hline S_{p}(p_{32}-p_{d}) \\ \hline \end{array}\right\} \qquad \{\xi\} = \left\{\begin{array}{|c|} \hline \xi_{1L} \\ \hline \xi_{1R} \\ \hline \xi_{2L} \\ \hline \xi_{2R} \\ \hline \xi_{3L} \\ \hline \xi_{3R} \\ \hline \xi_{4L} \\ \hline \xi_{4R} \\ \hline \xi_{p} \\ \hline \end{array}\right\}$$

Figure 5 Force and Displacement Vectors

$$
\rho_d c_d^2
\begin{bmatrix}
S_{1L}^2\left(\frac{1}{V_{42}}+\frac{1}{V_{11}}\right)-\frac{L_{1L}S_{1L}\omega^2}{C_d^2} & -\frac{S_{1R}S_{1L}}{V_{11}} & 0 & 0 & 0 & 0 & 0 & -\frac{S_{4R}S_{1L}}{V_{42}} \\
-\frac{S_{1R}S_{1L}}{V_{11}} & S_{1R}^2\left(\frac{1}{V_{11}}+\frac{1}{V_{12}}\right)-\frac{L_{1R}S_{1R}\omega^2}{C_d^2} & -\frac{S_{2L}S_{1R}}{V_{12}} & 0 & 0 & 0 & 0 & 0 \\
0 & -\frac{S_{2L}S_{1R}}{V_{12}} & S_{2L}^2\left(\frac{1}{V_{12}}+\frac{1}{V_{21}}\right)-\frac{L_{2L}S_{2L}\omega^2}{C_d^2} & -\frac{S_{2R}S_{2L}}{V_{21}} & 0 & 0 & 0 & 0 \\
0 & 0 & -\frac{S_{2R}S_{2L}}{V_{21}} & S_{2R}^2\left(\frac{1}{V_{21}}+\frac{1}{V_{22}}\right)-\frac{L_{2R}S_{2R}\omega^2}{C_d^2} & -\frac{S_{2R}S_{3L}}{V_{22}} & 0 & 0 & 0 \\
0 & 0 & 0 & -\frac{S_{3L}S_{2R}}{V_{22}} & S_{3L}^2\left(\frac{1}{V_{22}}+\frac{1}{V_{31}}\right)-\frac{L_{3L}S_{3L}\omega^2}{C_d^2} & -\frac{S_{3L}S_{3R}}{V_{31}} & 0 & 0 \\
0 & 0 & 0 & 0 & -\frac{S_{3R}S_{3L}}{V_{31}} & S_{3R}^2\left(\frac{1}{V_{31}}+\frac{1}{V_{32}}\right)-\frac{L_{3R}S_{3R}\omega^2}{C_d^2} & -\frac{S_{4L}S_{3R}}{V_{32}} & 0 \\
0 & 0 & 0 & 0 & 0 & -\frac{S_{4L}S_{3R}}{V_{32}} & S_{4L}^2\left(\frac{1}{V_{32}}+\frac{1}{V_{41}}\right)-\frac{L_{4L}S_{4L}\omega^2}{C_d^2} & -\frac{S_{4R}S_{4L}}{V_{41}} \\
-\frac{S_{4R}S_{1L}}{V_{42}} & 0 & 0 & 0 & 0 & 0 & -\frac{S_{4R}S_{4L}}{V_{41}} & S_{4R}^2\left(\frac{1}{V_{41}}+\frac{1}{V_{42}}\right)-\frac{L_{4R}S_{4R}\omega^2}{C_d^2}
\end{bmatrix}
$$

Figure 6 Matrix [A]

Figure 7 Gas Displacement Mode Associated with f_1

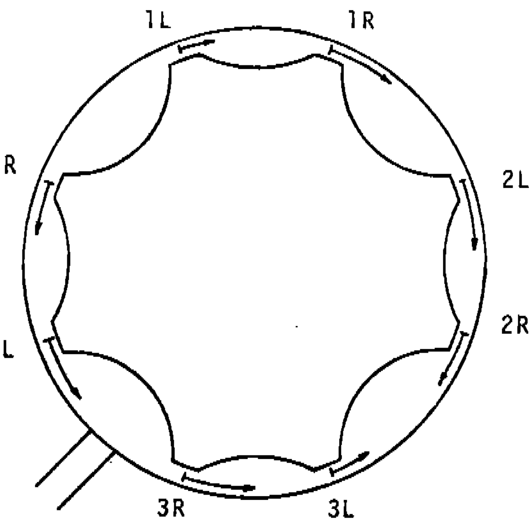

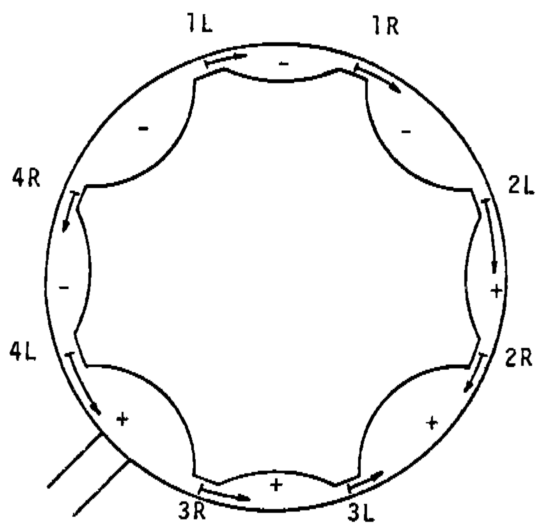

Figure 8 Gas Volume Displacement Mode Associated with f_1

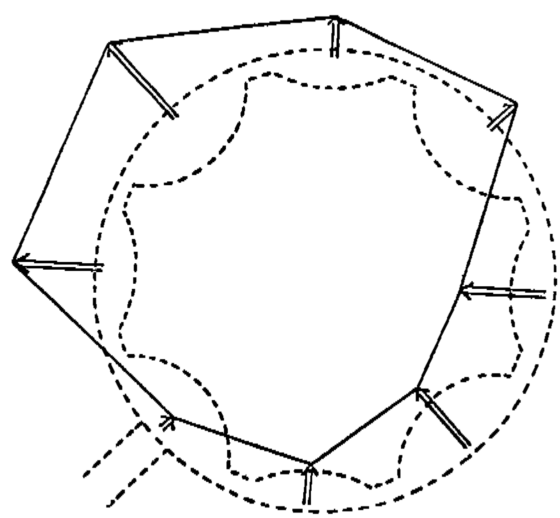

Figure 9 Pressure Mode Associated with f_1

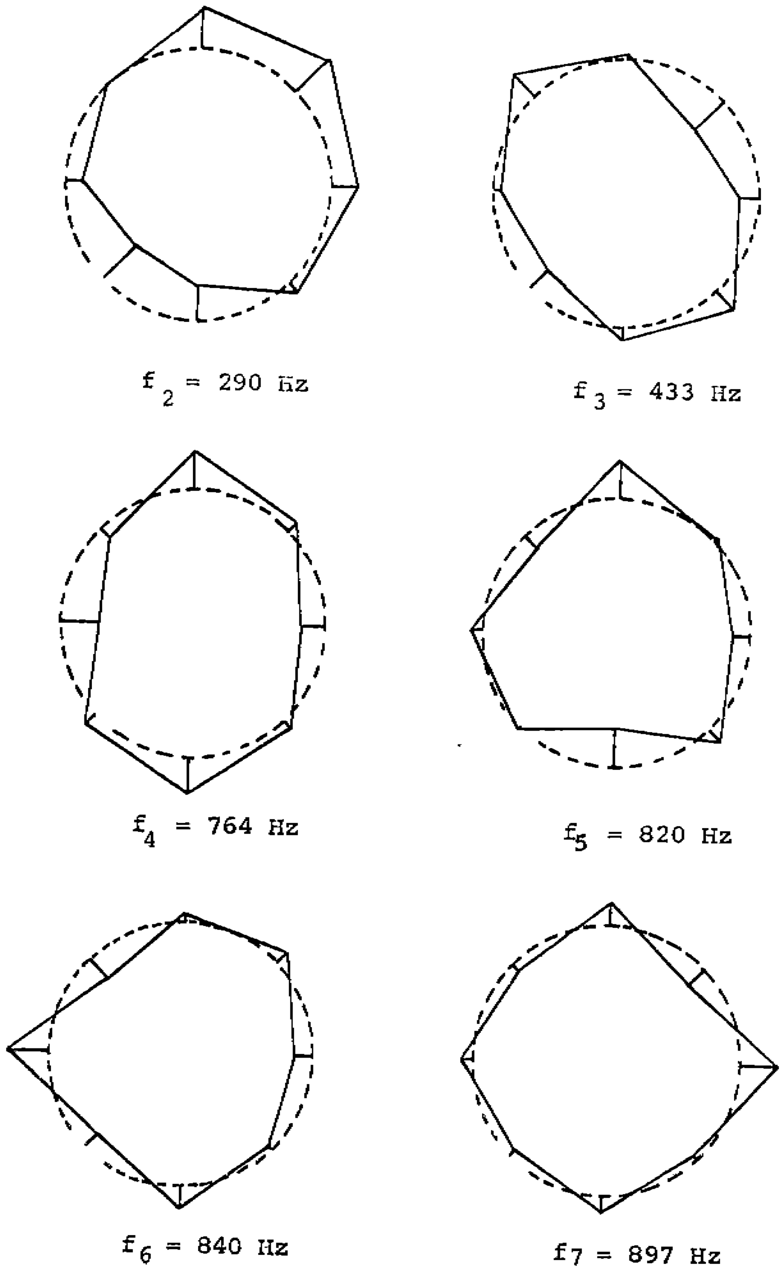

Figure 10 The Other Pressure Modes

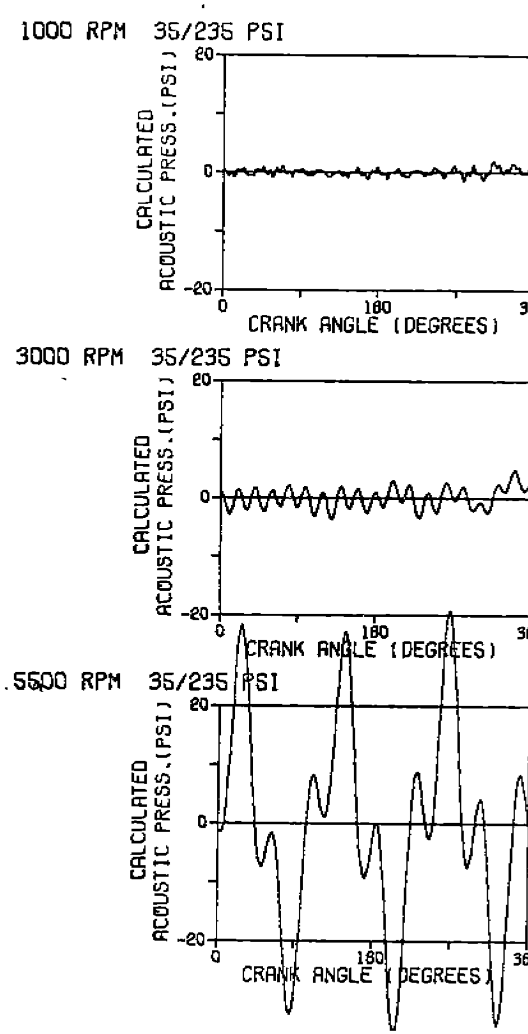

Figure 11 Pressures Above Cylinder 1

Harmonic of Running Speed
Which Excites Mode

Natural Frequency of Mode Excited

	267	290	434	764	820	840	897
1	16001	17405	26012	[illegible]	[illegible]	[illegible]	[illegible]
2	8001	8702	13006	[illegible]	[illegible]	[illegible]	[illegible]
3	5334	5802	8671	15290	[illegible]	16810	[illegible]
4	4000	4351	6503	11467	[illegible]	[illegible]	[illegible]
5	3200	3481	5202	9174	[illegible]	10086	[illegible]
6	2667	2901	4335	7645	[illegible]	8406	[illegible]
7	2286	2486	3716	6553	[illegible]	7204	[illegible]
8	2000	2176	3252	5734	[illegible]	6304	[illegible]
9	1778	1934	2890	5097	5465	5603	5978
10	1600	1740	2601	4587	4918	5043	5380
11	1455	1582	2365	4170	4471	4584	4891
12	1333	1450	2168	3822	4098	4202	4483
13	1231	1339	2001	3528	3783	3879	4138
14	1143	1243	1858	3276	3513	3602	3843
15	1067	1160	1734	3058	3279	3362	3587
16	1000	1088	1626	2867	3074	3152	3363
17	941	1024	1530	2698	2893	2966	3165
18	889	967	1445	2548	2732	2802	2989
19	842	916	1369	2414	2588	2654	2832
20	800	870	1301	2293	2459	2521	2690
21	762	829	1239	2184	2342	2401	2562
22	727	791	1182	2085	2235	2292	2445
23	696	757	1131	1994	2138	2193	2339
24	667	725	1084	1911	2049	2101	2242
25	640	696	1040	1835	1967	2017	2152
26	615	669	1000	1764	1892	1940	2069
27	593	645	963	1699	1822	1868	1993
28	571	622	929	1638	1756	1801	1921
29	552	600	897	1582	1696	1739	1855
30	533	580	867	1529	1639	1681	1793
31	516	561	839	1480	1586	1627	1735
32	500	544	813	1433	1537	1576	1681
33	485	527	788	1390	1490	1528	1630
34	471	512	765	1349	1446	1483	1582
35	457	497	743	1311	1405	1441	1537
36	444	483	723	1274	1366	1401	1494
37	432	470	703	1240	1329	1363	1454
38	421	458	685	1207	1294	1327	1416
39	410	446	667	1176	1261	1293	1379
40	400	435	650	1147	1230	1261	1345

Figure 12 Table of Critical Crank Speeds